ADVANCING EARTH AND SPACE SCIENCE

Geophysical Research Letters

RESEARCH LETTER

10.1029/2021GL093110

Key Points:

- The first numerical analysis of basal crevasse opening including ice shelf bending is presented
- Basal crevasses can be an order of magnitude wider than predicted by classical studies
- An analytic thin elastic plate description matches the numerical results in terms of crevasse width for a freely floating ice layer

Supporting Information:

Supporting Information may be found in the online version of this article.

Correspondence to:

W. R. Buck,
buck@ldeo.columbia.edu

Citation:

Buck, W. R., & Lai, C.-Y. (2021). Flexural control of basal crevasse opening under ice shelves. *Geophysical Research Letters*, *48*, e2021GL093110. https://doi.org/10.1029/2021GL093110

Received 23 FEB 2021
Accepted 24 MAR 2021

Flexural Control of Basal Crevasse Opening Under Ice Shelves

W. Roger Buck[1] and Ching-Yao Lai[2]

[1]Lamont-Doherty Earth Observatory of Columbia University, New York, NY, USA, [2]Department of Geosciences Program in Atmospheric and Oceanic Sciences, Princeton University, Princeton, NJ, USA

Abstract Classical analyses of basal crevasse opening do not account for the free surface of a floating ice layer. We describe a high-resolution numerical treatment of the opening of a single crevasse in a finite thickness elastic layer floating on an inviscid substrate. For low extensional stress (less than about half of the expected maximum for a freely floating shelf) the resulting crevasse height and width match previous studies. For larger magnitude applied extensional stresses, the new results predict basal crevasse widths an order of magnitude greater than the classical solution. An analysis using the thin-layer approximation shows that the greatly increased predicted width of basal crevasse opening results from layer bending. Given that the height and width of basal crevasses are non-linear functions of the stress experienced by an ice shelf, the new model results may enable better estimation of buttressing stresses for different parts of ice shelves.

Plain Language Summary Basal crevasses are water filled cracks the cut through much of the ice shelves and so contribute to their breakup. A new analysis shows that basal crevasses can break through significantly more of a floating ice layer than previous models that could not consider the bending of the ice layer. This more consistent approach suggests that basal crevasses can be an order of magnitude wider than estimated by the earlier studies. A simple analytic description of flexure of ice layers correctly predicts the maximum width of basal crevasses.

1. Introduction

The rate of flow and disintegration of ice shelves may depend critically on the opening of crevasses cutting the shelf (Banwell et al., 2013; Clerc et al., 2019; Lai et al., 2020; Robel & Banwell, 2019; Scambos et al., 2009). Ice shelves can retard the flow of adjacent grounded ice sheets (Fürst et al., 2016; Schoof, 2007). Therefore, crevassing processes can affect the rate of sea level rise on a warming Earth (e.g., DeConto & Pollard, 2016; Pollard et al., 2015). Water-filled basal crevasses may cut through much of a floating ice layer and so may more strongly affect large-scale shelf deformation than the relatively shallow opening dry surface crevasses (e.g., Bassis & Ma, 2015). Previous analyses of crevasse opening (e.g., Weertman, 1973) assumed no deflection of the surface so that a semi-analytic dislocation approach could be used, but advances in numerical methods make possible a more realistic treatment of crevasse opening.

Basal crevasses are water-filled tensile cracks. Since floating ice shelves should be under horizontal tension those cracks should be approximately vertical and radar images confirm this prediction (Figure S1; Luckman et al., 2012; McGrath, 2012). The opening of such cracks reduces the tension in the base of the ice layer and increases tension above the crack (Weertman, 1973). The rate of ice flow depends non-linearly on the applied stress (e.g., Glen, 1952), with a given increase in stress difference producing a correspondingly large increase in flow rate. Thus, the increase of stress in the shallow part of an ice shelf due to crevasse opening could greatly increase the rate of ice flow above the crevasse, as shown by Bassis and Ma (2015).

Previous analyses of basal crevasse opening do not fully treat the bending of a floating, finite thickness layer and so may underestimate the height and width of a basal crevasse. The classical treatment of crevasse opening in an elastic half-space (e.g., Weertman, 1973) predicts such a narrow opening that Weertman (1980) considered that crevasses would largely freeze for all but the thickest ice shelves.

In this paper, we analyze the opening of a water-filled basal crevasse in a floating elastic ice layer of uniform thickness (Figure 1). The numerical model boundary conditions only differ from those assumed by

10.1029/2021GL093110

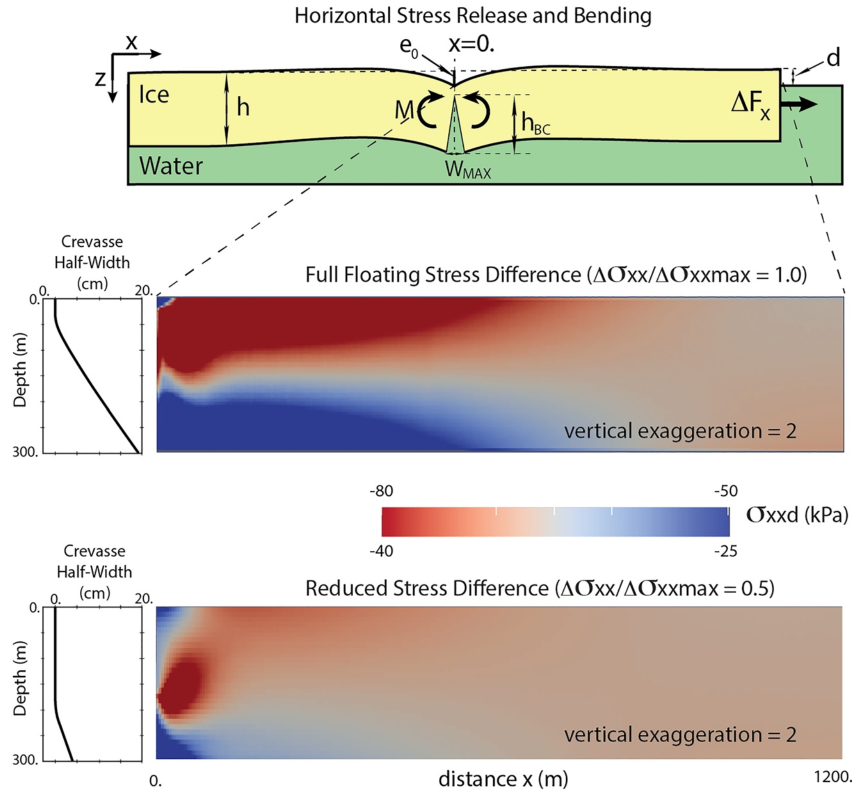

Figure 1. Top panel schematically illustrates how basal crevasse opening to a height h_{BC} could produce layer bending. The ice layer is subject to an extensional force $\Delta F_x = \left(h \Delta \sigma_{xx}\right)$ applied far from the site of the crevasse opening. The pressure of water in the crevasse produces a bending moment M that increases the maximum width w_{MAX} of the crevasse. The bottom two panels show results of numerical determinations of horizontal deviatoric stress $\left(\sigma_{xxd}\right)$ during basal crevasse opening for the radiolabeled values of the vertically uniform extensional stress ($\Delta \sigma_{xx}$) applied to the right side of the model domain (see text). For the "full floating stress" case the extensional stress magnitude is described in the text. For the lower plot, the extensional stress is assumed to be reduced by half due to buttressing at the sides of the ice shelf. In both cases, Young's modulus was set to 10^9 Pa. The horizontal opening of the respective model crevasses is shown to the left of the stress plots.

Weertman (1973) in that the ice layer is taken to have a finite thickness. We then show derive an approximate thin plate analytic description of basal crevasse opening that shows how flexure explains the additional crevasse width. Before describing our treatment of basal crevasse opening for a floating ice layer we describe two classical treatments of crevasse opening.

1.1. Previous Analyses of Crevasse Opening

The height of the crevasse opening was discussed by Nye (1955) under the assumption that the opening does not affect stresses in ice. He argues that the tip of the crevasse is at the depth where the pressure P_f of fluid in the crevasse equals the horizontal full stress σ_{xx} there. Nye (1955) assumed that the vertical stress equals the lithostatic stress in the column of ice so that the full horizontal stress is:

$$\sigma_{xx}\left(z\right) = \rho_i g z - \Delta \sigma_{xx} \tag{1}$$

where $\Delta \sigma_{xx}$ is an applied tensional stress and z is the depth below the surface of a horizontally uniform ice layer, ρ_i is ice density, and g is the acceleration of gravity. For an ice layer of thickness h floating on the water density ρ_w the fluid pressure in a basal crevasse is:

$$P_f\left(z\right) = \rho_i g h - \rho_w g\left(h - z\right), for\ h < z < d \tag{2}$$

10.1029/2021GL093110

where d is the depth to the water below the top of a floating ice sheet of thickness h, as pictured in Figure S2, and is:

$$d = h\frac{(\rho_w - \rho_i)}{\rho_w} \tag{3}$$

where ρ_w is the density of water. With this pressure in the crevasse, Nye's assumption implies that that the height of a basal crevasse is:

$$h_B^{Nye} = \frac{\Delta\sigma_{xx}}{(\rho_w - \rho_i)g}. \tag{4}$$

Nye (1955) noted that the assumption that crevasse opening does not change the horizontal stress in the ice should only hold if crevasses are very closely spaced. He suggested that the opening of a single crevasse should affect stresses at the crack tip so that estimating the crevasse height would require a more involved analysis.

The challenge of analyzing the opening of a single crevasse in an ice layer was taken up by Weertman (1973) who simulated the effect of the crack opening using a series of dislocations in an elastic half-space. He followed Nye (1955) in assuming that the position of the crack tip would be the place where the pressure in the crack equaled the horizontal stress in the ice. The Weertman (1973) solution predicts that both surface and basal crevasses would open much farther than predicted by Nye (1955). For a basal crevasse height that is small compared to the ice layer thickness he found a height:

$$h_B^{Weertman} \approx 1.05\left(\frac{\pi}{2}\right)h_B^{Nye} \approx 1.65 h_B^{Nye} \tag{5}$$

which is the same as crevasse height in an infinite elastic half-space predicted from linear elastic fracture mechanics (LEFM; van der Veen, 1998) with zero fracture toughness (see Figure S3).

Using a standard estimate of the maximum horizontal tension in a floating layer, Weertman (1973) estimated the maximum height of a crevasse opening for the case of a crevasse far from the edge of such a layer. His analysis computed the force exerted by water on the side of the layer and because that is insufficient to support the load of the ice, the layer will be under tension. The maximum difference between the water pressure and the lithostatic stress in the ice occurs at depth d below the surface of the ice (Figure S2) and is:

$$\Delta P_{MAX} = \rho_i g d = gh\frac{\rho_i}{\rho_w}(\rho_w - \rho_i) \tag{6}$$

Far from the edge of the ice layer, this extensional force should result in a uniform reduction in the horizontal stress σ_{xx} relative to the vertical stress σ_{zz}. The horizontal stress is then given by Equation 1 with

$$\Delta\sigma_{xx} = \Delta\sigma_{xxMAX} = \frac{1}{2}gh\frac{\rho_i}{\rho_w}(\rho_w - \rho_i) \tag{7}$$

We term this the maximum floating stress difference since it could be reduced by any "buttressing stresses" at the sides of an ice shelf. Using this value of stress difference and that $\rho_w = 1000\ kg/m^3$ and $\rho_i = 900\ kg/m^3$ in Equation 4, Nye (1955) would predict $h_B^{Nye} = 0.45h$ while Weetman's (1973) analysis (Equation 5) predicts a basal crevasse height of 0.74 h.

The width of a crevasse can be precisely estimated for a crack opening in a half-space. For the extensional stress in a freely floating 300 m thick ice layer with the densities assumed above and with typical laboratory-measured elastic properties for ice (Young's modulus of ∼10^{10} Pa and a Poisson's ratio of 0.25; Gammon et al., 1983) the maximum predicted basal crevasse width would be ∼0.5 cm (Weertman, 1973). As with magma freezing in a dike, the time to freeze should scale with the inverse square of the crevasse width (e.g., Turcotte & Schubert, 2014). As noted by Weertman (1980) accounting for the latent heat of solidification such a narrow crack could freeze on a time scale of minutes if it intrudes ice a few degrees below zero. Thus, water might freeze in a crack after propagating only a short distance.

Weertman (1980) assumed that a basal crevasse would only stay open if it would not freeze in the time required for enough ductile flow of the ice above the crevasses to significantly widen the crevasse. For typical ice rheologic parameters, he estimated that only basal crevasses in a freely floating layer thicker than ∼1,000 m would be wide enough to stay open and not freeze completely. This seems at odds with radar observations that detect basal crevasses under much thinner ice shelves (Luckman, 2012; McGrath, 2012)

2. Basal Crevasse Opening for a Floating Ice Layer of Finite Thickness

Weertman (1973) noted that effects related to the free surface of a floating ice layer not treated in his analysis could affect basal crevasse opening. Thus, we performed a series of numerical simulations using much the same boundary conditions as Weertman (1973) except that the floating layer was taken to have a free surface. As in mentioned inprevious studies of surface crevasses opening (Qin et al., 2007) and magma filled dike opening (Bialas et al., 2010; Qin & Buck, 2008), the numerical code FLAC (Cundall, 1989) was used to compute the stresses produced by the opening of a crevasse in a 2D floating elastic layer.

An elastic layer at least 12 times wider than its uniform height h was loaded on the right side with horizontal stress given by Equation 1 with particular values of the horizontal stress difference $\Delta\sigma_{xx}$ (Figure 1). The layer surface was stress-free and the other three sides were taken to be shear stress-free. The base of the layer was treated as a Winkler foundation simulating floating on an inviscid fluid of density equal to the density of water. As above, the water density was set to $\rho_w = 1{,}000\ kg\ /\ m^3$ and the ice density was $\rho_i = 900 kg\ /\ m^3$. For all cases, the Poisson's ratio was set to 0.25.

Since the opening of a vertical crevasse should be symmetric only one side was treated numerically. The left side of the model domain was assumed to be the site of the basal crevasse opening. From the surface to the depth of the assumed top of the crevasse, z_B (Figure S2), the horizontal displacement was set to zero. Between $z = z_B$ and $z = h$, the horizontal stress was set to the value of the water pressure given by Equation 2. The depth from the top of the crevasse was varied until the horizontal stress at the top of the layer approximately equaled the water pressure at that depth. If the trial value of z_B was too large (small) the horizontal stress was greater (less) than the water pressure (using the geologic convention that compression is positive). The size of the square elements used was decreased until the effect on crevasse height was less than a few percent. The finest scale models were done with 60 elements vertically and 720 horizontally.

2.1. Numerical Results

Three parameters were varied in a series of model cases: the layer thickness h, Young's modulus E, and the applied extensional stress difference $\Delta\sigma_{xx}$. The stress difference was varied between zero and the maximum value for a freely floating layer given by Equation 7. Figure 2a shows the computed height of basal crevasses as a function of the applied stress ratio $\Delta\sigma_{xx}\ /\ \Delta\sigma_{xxMAX}$. For these cases the ice layer thickness was 300 m and Young's modulus E was set to 10^9 Pa. Also, shown are the predictions of the crevasse heights for the Nye (1955) and Weertman (1973) approximations. For very small values of the stress ratio, the numerical results equal the Weertman (1973) results but they diverge significantly $\Delta\sigma_{xx}\ /\ \Delta\sigma_{xxMAX} \gtrsim 0.5$.

For the maximum floating stress, the non-dimensional basal crevasse height (h_B/h) for the finite thickness layer is ∼0.9 compared to the value predicted for a half-space of ∼0.74 given by Weertman (1973). Increasing the layer depth from 100 to 1,000 m decreases the maximum dimensional basal crevasse height (h_B/h) by a few percent. Likewise, increasing Young's modulus by a factor of 10 increases the maximum predicted basal crevasse height by several percent.

The width of the bottom of the basal crevasses as a function of the stress ratio is shown in Figure 2b. For small values of the applied stress, the numerical widths are very close to the half-space solution. However, for large values of the applied stress, the width for the finite layer thickness calculations is up to 10 times

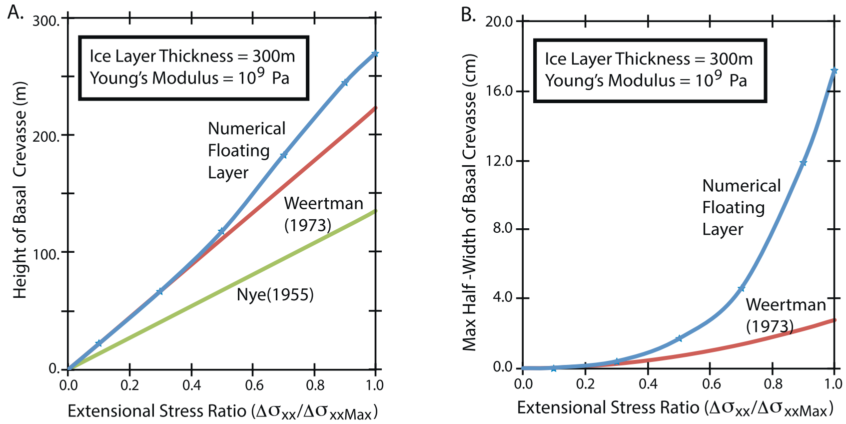

Figure 2. (a) Results of calculated basal crevasse height versus non-dimensional extensional stress from our 2D numerical treatment of a floating elastic ice layer (blue) for a Poisson's ratio of 0.25 and the indicated ice layer thickness and Young's modulus. Also shown are estimates based on an elastic half-space approximation (Weertman, 1973, red) or for an infinite number of laterally adjacent crevasses (Nye, 1955, green). (b) Predicted maximum half-width of the basal crevasses for the same numerical cases as in (a) and for the elastic half-space solution with the same elastic properties as in (a) All results assume an ice density of 900 kg/m^3, a water density of 1,000 kg/m^3.

larger than for the half-space cases for a reasonable value of Young's modulus. Unlike for the crevasse height, the width depends strongly on Young's modulus as can be seen in Figure 3.

The pattern of stress changes for the finite thickness layer is fundamentally different depending on the applied stress. Figure 1 shows horizontal deviatoric stresses $\left[\sigma_{xxd} = \sigma_{xx} - \left(\sigma_{xx} + \sigma_{zz}\right)/2\right]$ for two of the numerical cases after basal crevasse opening. In both cases, the region laterally adjacent to the open crevasse shows a marked increase in the horizontal stress (i.e., the stresses become more compressive). Had the crack been opening in an elastic half-space the region of significant stress change would be roughly twice as wide as the height of the crevasse (e.g., Weertman, 1980). This is essentially, what is seen in the case $\Delta\sigma_{xx} / \Delta\sigma_{xxMAX} = 0.5$ where the crevasse opens to a height of ~0.35 h. When the applied stress ratio was equal to 1 the region of stress changes are many times wider than the crevasse height. As shown in Figures 2b and 3 the crevasse width was also many times larger than expected for a crack in a half-space. Crack opening as a function of depth is plotted in Figure 1.

2.2. Analytic Model of Basal Crevasse Opening for a Freely Floating Ice Shelf

The numerical model shows that the width of the crevasse opening for a finite thickness, freelyfloating elastic layer ($\Delta\sigma_{xx} / \Delta\sigma_{xxMAX} = 1$) can be many times larger than the opening under the same stress applied to a half-space (Figure 2). To elucidate the reason for this great difference in predicted width we consider a simple model of flexure in response to stress changes on crevasse opening. Many authors have noted that the existence of a free end of an ice shelf should result in flexure of that layer (Logan et al., 2013; MacAyael and Sergienko, 2013; MacAyal et al., 2015; Reeh, 1968; Sandwell et al., 2004; Schmeltz et al., 2002). Here, we apply thin elastic plate flexure theory (e.g.,Watts, 2001) to try to estimate the extra opening of a basal crevasse due to the bending of a floating ice layer. The only case considered is where the applied stress equals the maximum value due to free floatation as given by Equation 7.

As with the numerical model described above, a basal crevasse is assumed to open far from the shelf edge where the initial, pre-opening, horizontal stress distribution with depth is described by Equation 1. Tensile fracturing allows water to apply hydrostatic pressure to the sides of the opening crevasse. At the base of the sheet, the horizontal stress will then equal the vertical stress so the horizontal stress there would increase by $\frac{1}{2}\Delta P_{MAX}$ on the bottom crevasse opening.

Consistent with our numerical results for the case of $\Delta\sigma_{xx} / \Delta\sigma_{xxMAX} = 1.0$ a basal crevasse is assumed to open from the base of the ice shelf to a depth d from the surface, where d is the freeboard of the ice shelf

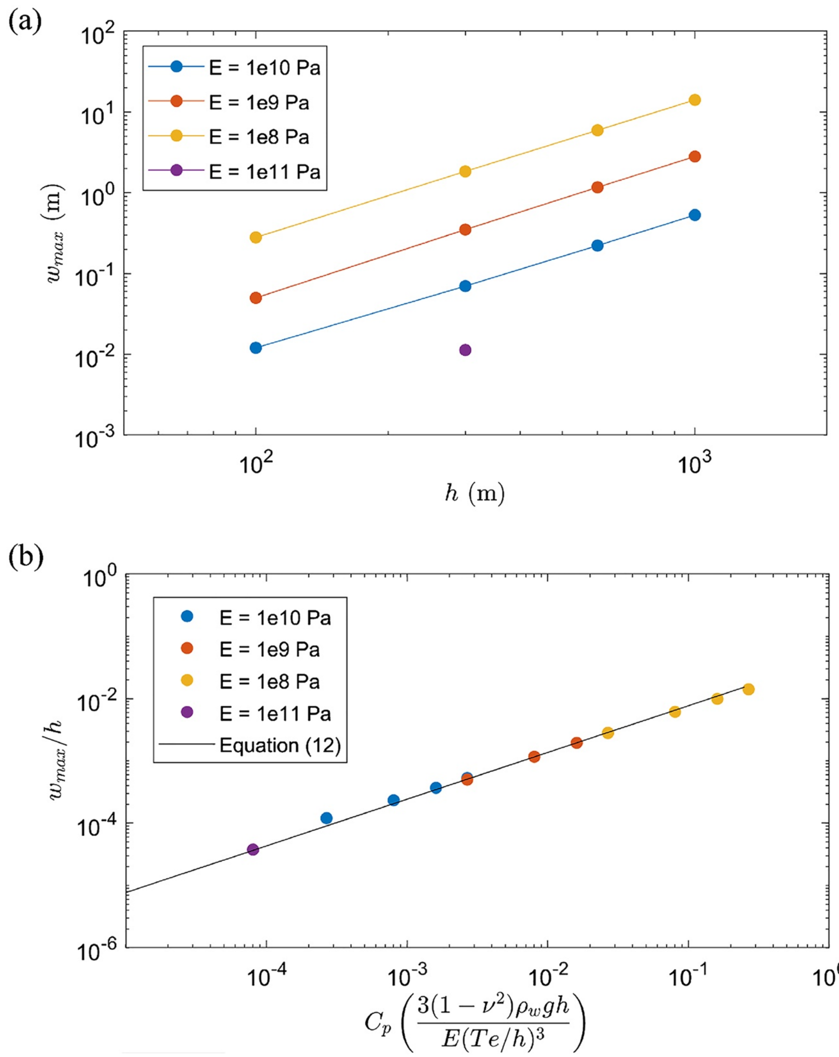

Figure 3. Comparison between analytic (lines) and numerical (colored dots) estimates of the maximum half-width of a basal crevasse for 13 numerical cases with different values of the layer thickness and Young's modulus The non-dimensional extensional stress was taken to be 1 (*i.e.* $\Delta\sigma_{xx} / \Delta\sigma_{xxMAX} = 1$)., meaning the stress equaled the full floating stress. (a) Shows the log of the half width versus log of the layer thickness for four different Young's moduli. (b) Shows that the rescaled crevasse width and rescaled layer thickness for four different Young's moduli collapse onto a universal curve, and exhibit good agreements with the analytical prediction (Equation 12) without any fitting parameters. The slope of the black line is ¾. (Fixed parameters for all points: $\nu = 0.25$, $\rho_w = 1000\, kg / m^3$, $\rho_i = 900\, kg / m^3$, $Te = h$).

given by Equation 3. The total horizontal stress in the layer before the opening of a crevasse σ_{xx}^0 is given by Equation 1 with $\Delta\sigma_{xx} = \Delta\sigma_{xxMAX}$. After the crevasse opens the new horizontal stress σ_{xx}^1 from depth d to the base of the ice sheet the horizontal stress changes to equal the water pressure $\left(= \rho_w g\left(z-d\right)\right)$. Continuity of horizontal stress is required across the top of the crevasse at depth $z = d$. Also, bending should result in no change in the average horizontal stress in the unbroken region above the open crevasse (e.g., Bodine et al., 1981). The simplest way to meet these requirements is to have σ_{xx}^1 equal zero from the surface to $z = d$. Then the change in horizontal stress after the opening of the basal crevasse is

$$\begin{aligned} \sigma_{xx}^1(z) - \sigma_{xx}^0(z) &= \Delta P_{MAX}\left(\frac{1}{2} - \frac{z}{d}\right) \ for\ z < d \\ \sigma_{xx}^1(z) - \sigma_{xx}^0(z) &= \Delta P_{MAX}\left(\frac{z-d}{h-d} - \frac{1}{2}\right) \ for\ d < z < h. \end{aligned} \tag{8}$$

10.1029/2021GL093110

Figure S4 shows the distribution of initial stress in the layer and the change in stress after the opening of a crevasse. This distribution of stress changes implies a moment applied to the vertical edge of the crevasse and the region above the crevasses tip that can be expressed as:

$$M = \int_0^h \left[\sigma_{xx}^1(z) - \sigma_{xx}^0(z) \right] z dz = \frac{\Delta P_{MAX}}{12}\left(h^2 - 2dh\right) \tag{9}$$

Assuming $\rho_i / \rho_w = 0.9$ means that $d = h/10$ so that $M = \frac{\Delta P_{MAX}}{15} h^2$. The moment should cause bending of the ice adjacent to the site of the basal crevasse. Thin plate flexure theory is a useful way to estimate the amplitude and wavelength of the vertical displacement of the ice layers. Though the ice is not completely cut by the basal crevasse, assuming the plate is broken there allows the derivation of an analytic description of the displacement. For a semi-infinite broken thin elastic plate, the vertical displacement (positive down) above the basal crevasse due to a moment M applied at $x = 0$ is:

$$e_0 = \frac{2M}{\alpha^2 \rho_w g} \tag{10}$$

where α is the flexure parameter defined below. The crevasse half-width should approximately equal the slope of the surface at $x = 0$ (which can be shown to equal $\frac{2e_0}{\alpha}$) times the depth below the top of the crevasse. Thus, the maximum full width of the basal crevasse is $w_{\max} = (4e_0 / \alpha)(h - d)$.

The results of the surface deflection and crevasses opening width strongly depend on the ratio α/h. The thickness h is relatively easy to measure for in the ice shelf, but the value of the flexure parameter is much harder to constrain. Thin elastic plate theory (Turcotte & Schubert,2014) implies that α is related to the effective elastic thickness, Te, of the layer as:

$$\alpha = \left[\frac{E(Te)^3}{3(1 - \nu^2)\rho_w g} \right]^{1/4} \tag{11}$$

where E is Young's modulus and ν is Poisson's ratio. Assuming that the layer bends in a purely elastic fashion (with no yielding) then $Te = h$. With $E = 10^{10}$ Pa, $\nu = 0.25$ and for $h = 300$ m this gives $\alpha/h \sim 6$. Combining Equations 3, 6, 9, 10 and 11 yields

$$\frac{w_{\max}}{h} = C_\rho \left(\frac{h}{\alpha}\right)^3 = C_\rho \left(\frac{3(1 - \nu^2)\rho_w g h}{E(Te / h)^3} \right)^{\frac{3}{4}} \tag{12}$$

$$\text{where } C_\rho \equiv \frac{2}{3}\left(\frac{\rho_i}{\rho_w}\right)^2 \left(1 - \frac{\rho_i}{\rho_w}\right)\left(2\frac{\rho_i}{\rho_w} - 1\right).$$

To test our analytical model, the results of 13 numerical experiments with $\Delta\sigma_{xx} / \Delta\sigma_{xxMAX} = 1$ (i.e., a freely floating layer) of basal crevasse half-width as a function of layer thickness for a range of Young's moduli and layer thicknesses are shown in Figure 3a. Four different Young's modulus values are shown by the four curves. We then non-dimensionalize the axis of Figure 3a according to Equation 12 and show that the data for different Young's modulus collapses (Figure 3b) onto the analytical solution (Equation 12) where $Te = h$. The collapse of dimensionless data on Figure 3b shows the excellent agreement between the numerical simulation and the analytical solution (Equation 12) for Young's modulus varying across four orders of magnitudes.

Note that the cases shown in Figure 3 consider Young's moduli both lower and higher than measured or estimated values (Gammon et al., 1983; Nimmo, 2004). The computer time for obtaining a reliable (converged) solution using our explicit numerical formulation is found to depend on flexural wavelength. For the lowest values of the Youngs modulus and so the shortest wavelengths the numerical calculations converge in less than a CPU hour, while for cases with the highest values of E convergence can take a CPU day. Thus, we only did one numerical case with a very high value of Young's modulus.

For brittle layers, like rock or ice, bending causes yielding that will make Te smaller than layer thickness h. Theory predicts that the Te should be a strong function of the curvature of a plate (e.g., Buck, 1988) and geologically realistic bending can result in the reduction of Te by an order of magnitude (Choi & Buck, 2012). Nimmo (2004) complied data on the flexing of ice shelves by tidal loads and concluded that brittle failure due to those loads reduces Te by ~30%–50%. In our simulations, we did not allow brittle yielding and considered only the elastic behavior of an ice layer.

3. Discussion and Conclusions

The numerical study of basal crevasse opening in an elastic layer described here differs significantly from previous models that do not account for the finite thickness and free surface of a floating ice shelf. The height of the crevasse is more sensitive to the extensional stress in the layer than predicted by earlier studies. The new results predict that a basal crevasse can be an order of magnitude wider than predicted for earlier studies that consider a crack opening in an elastic half-space solution.

An analysis using the thin-layer approximation shows that the greatly increased width of basal crevasse opening for extensional stresses expected in a freely floating ice shelf (i.e., when buttressing stress is minimal) stress results from layer bending. The bending is driven by changes in the horizontal stresses along and above a newly opened crevasse. Analytic predictions of the width of the base of a basal crevasse closely match the predictions of the numerical model and show the same nonlinear dependence on the layer thickness and Young's modulus assumed for the ice.

The time to freeze a water-filled crevasse depends on the square of its width just as it does for magma solidifying in a dike (e.g., Turcotte & Schubert, 2014). The new results suggest that a basal crevasse may take as much as 100 times as long to freeze as predicted by the classical analysis. Thus, a basal crevasse may be more likely to propagate through much of an ice shelf before freezing would arrest propagation. The wide crack may then stay open long enough for ductile flow of the region above the open crevasse to further widen the crack and so keep it open as envisioned by Weertman (1980). This would result in the kind of localized thinning of the ice above a crevasse discussed in previous studies (e.g., Bassis & Ma, 2015). We note that whether the ocean within basal crevasses under the ice shelves can freeze is an active area of research (e.g., the ICEFIN project). Here we focus on the widening of basal crevasse due to ice-shelf deformation that can contribute to the increase of freezing time.

The lateral confinement of ice shelves provides buttressing that can reduce the extensional stress experienced by a region of an ice shelf. Lower values of the ratio of extensional stress to the maximum expected for a freely floating layer (e.g., $\Delta\sigma_{xx}$ / $\Delta\sigma_{xxMAX}$) can be thought of as representing stronger buttressing (Fürst et al., 2016). Near the edge of an ice shelf, this stress ratio should approach 1.0 and so the basal crevasses should be the tallest and widest. In areas where the sides of a flowing ice shelf are confined, so shear stresses reduce downstream extensional stresses, we expect that basal crevasses should be shorter (e.g., Jezek, 1984).

The present study implies that basal crevasses subject to free-floating stresses open significantly wider than estimated by previous studies. Higher-resolution models than those employed here will be needed to quantify the precise level of extensional stress needed for the complete breaking of an ice layer, but it appears to be only slightly larger than the free-floating stress.

The numerical approach used here can easily be applied to cases where the viscous and brittle rheology of ice is included. Future work should consider the full 2D treatment of the development of a series of crevasses, including the thermal evolution of that system.

Data Availability Statement

Figure S1 has been obtained from CReSIS (2020) Radar Depth Sounder, Lawrence, Kansas, USA. Digital Media. http://data.cresis.ku.edu/. The numerical code we used for these model runs can be found at https://bitbucket.org/tan2/flac/src/default/.

Acknowledgments
The authors thank Tim Creyts, Jonny Kingslake and two anonymous reviewers for helpful suggestions. C.-Y. L. thanks the Lamont-Doherty Earth Observatory for funding through the Lamont Postdoctoral Fellowship.

References

Banwell, A. F., MacAyeal, D. R., & Sergienko, O. V. (2013). Breakup of the Larsen B Ice Shelf triggered by chain reaction drainage of supraglacial lakes. *Geophysical Research Letters*, *40*(22), 5872–5876. https://doi.org/10.1002/2013gl057694

Bassis, J. N., & Ma, Y. (2015). Evolution of basal crevasses links ice shelf stability to ocean forcing. *Earth and Planetary Science Letters*, *409*, 203–211. https://doi.org/10.1016/j.epsl.2014.11.003

Bialas, R. W., Buck, W. R., & Qin, R. (2010). How much magma is required to rift a continent? *Earth and Planetary Science Letters*, *292*(1–2), 68–78. https://doi.org/10.1016/j.epsl.2010.01.021

Bodine, J. H., Steckler, M. S., & Watts, A. B. (1981). Observations of flexure and the rheology of the oceanic lithosphere. *Journal of Geophysical Research*, *86*(B5), 3695–3707. https://doi.org/10.1029/jb086ib05p03695

Buck, W. R. (1988). Flexural rotation of normal faults. *Tectonics*, *7*(5), 959–973. https://doi.org/10.1029/tc007i005p00959

Choi, E., & Buck, W. R. (2012). Constraints on the strength of faults from the geometry of rider blocks in continental and oceanic core complexes. *Journal of Geophysical Research*, *117*. https://doi.org/10.1029/2011JB008741

Clerc, F., Minchew, B. M., & Behn, M. D. (2019). Marine ice cliff instability mitigated by slow removal of ice shelves. *Geophysical Research Letters*, *46*(21), 12108–12116. https://doi.org/10.1029/2019gl084183

CReSIS. (2020). *Radar depth Sounder*. Digital Media. http://data.cresis.ku.edu/

Cundall, P. A. (1989). Numerical experiments on localization in frictional materials. *Ingenieur-Archiv*, *59*(2), 148–159. https://doi.org/10.1007/bf00538368

DeConto, R. M., & Pollard, D. (2016). Contribution of Antarctica to past and future sea-level rise. *Nature*, *531*(7596), 591–597. https://doi.org/10.1038/nature17145

Fürst, J. J., Durand, G., Gillet-Chaulet, F., Tavard, L., Rankl, M., Braun, M., et al. (2016). The safety band of Antarctic ice shelves. *Nature Climate Change*, *6*, 5, 479–482. https://doi.org/10.1038/nclimate2912

Gagliardini, P. H., Kiefte, H., Clouter, M. J., & Denner, W. W. (1983). Elastic constants of artificial and natural ice samples by Brillouin spectroscopy. *Journal of Glaciology*, *29*(103), 433–460. https://doi.org/10.3189/s0022143000030355

Glen, J. W. (1952). Experiments on the deformation of ice. *Journal of Glaciology*, *2*(12), 111–114. https://doi.org/10.1017/s0022143000034067

Jezek, K. C. (1984). A modified theory of bottom crevasses used as a means for measuring the buttressing effect of ice shelves on inland ice sheets. *Journal of Geophysical Research*, *89*(B3), 1925–1931. https://doi.org/10.1029/jb089ib03p01925

Lai, CY., Kingslake, J., Wearing, M. G., Chen, P. C., Gentine, P., Li, H., et al. (2020). Vulnerability of Antarctica's ice shelves to meltwater-driven fracture. *Nature*, *584*(7822), 574–578. https://doi.org/10.1038/s41586-020-2627-8

Logan, L., Catania, G., Lavier, L., & Choi, E. (2013). A novel method for predicting fracture in floating ice. *Journal of Glaciology*, *59*(216), 750–758. https://doi.org/10.3189/2013JoG12J210

Luckman, A., Jansen, D. Kulessa, B., Kulessa, B., King, E. C. & Sammonds, P. &, Benn, D.I. (2012). Basal crevasses in Larsen C Ice Shelf and implications for their global abundance, *The Cryosphere*, *6*, 1, 113–123, https://doi.org/10.5194/tc-6-113-2012

MacAyeal, D. R., & Sergienko, O. V. (2013). The flexural dynamics of melting ice shelves. *Annals of Glaciology*, *54*. https://doi.org/10.3189/2013AoG63A2561

MacAyeal, D. R., Sergienko, O. V., & Banwell, A. F. (2015). A model of viscoelastic ice-shelf flexure. *Journal of Glaciology*, *61*(228), 635–645. https://doi.org/10.3189/2015jog14j169

McGrath, D., Steffen, K., Scambos, T., Rajaram, H., Casassa, G., & Rodriguez Lagos, J. L. (2012). Basal crevasses and associated surface crevassing on the Larsen C ice shelf, Antarctica, and their role in ice-shelf instability. *Annals of Glaciology*, *58*. https://doi.org/10.3189/2012AoG60A005

Nimmo, F. (2004). What is the Young's modulus of ice? Europa's icy shell meeting, *Europa's Icy Shell, LPI Contribution1195, 7005*. Houston, Texas: Lunar and Planetary Institute.

Nye, J. F. (1955). Comments on Dr. Loewe's letter and notes on crevasses. *Journal of Glaciology*, *2*(17), 512–514. https://doi.org/10.3189/s0022143000032652

Pollard, D., DeConto, R. M., & Alley, R. B. (2015). Potential Antarctic ice sheet retreat driven by hydrofracturing and ice cliff failure. *Earth and Planetary Science Letters*, *412*, 112–121. https://doi.org/10.1016/j.epsl.2014.12.035

Qin, R., Buck, W., & Germanovich, L. (2007). Comment on "Mechanics of tidally driven fractures in Europa's ice shell" by Lee S., Pappalardo R. T., and Makris N. C. [2005. Icarus 177, 367-379]. *Icarus*, *189*(2), 595–597. https://doi.org/10.1016/j.icarus.2007.01.013

Qin, R., & Buck, W. R. (2008). Why meter-wide dikes at oceanic spreading centers? *Earth and Planetary Science Letters*, *265*(3–4), 466–474. https://doi.org/10.1016/j.epsl.2007.10.044

Reeh, N. (1968). On the calving of ice from floating glaciers and ice shelves. *Journal of Glaciology*, *7*(50), 215–232. https://doi.org/10.3189/s0022143000031014

Robel, A. A., & Banwell, A. F. (2019). A speed limit on ice shelf collapse through hydrofracture. *Geophysical Research Letters*, *46*(21), 12092–12100. https://doi.org/10.1029/2019gl084397

Sandwell, D., Rosen, P., Moore, W., & Gurrola, E. (2004). Radar interferometry for measuring tidal strains across cracks on Europa. *Journal of Geophysical Research*, *109*. https://doi.org/10.1029/2004JE002276

Scambos, T., Fricker, H. A., Liu, C.-C., Bohlander, J., Fastook, J., Sargent, A., et al. (2009). Ice shelf disintegration by plate bending and hydro-fracture: satellite observations and model results of the 2008 Wilkins ice shelf break-ups. *Earth and Planetary Science Letters*, *280*(1–4), 51–60. https://doi.org/10.1016/j.epsl.2008.12.027

Schmeltz, M., Rignot, E., & MacAyeal, D. (2002). Tidal flexure along ice-sheet margins: comparison of InSAR with an elastic-plate model. *Annals of Glaciology*, *34*, 202–208. https://doi.org/10.3189/172756402781818049

Schoof, C. (2007). Ice sheet grounding line dynamics: Steady states, stability, and hysteresis. *Journal of Geophysical Research*, *112*. https://doi.org/10.1029/2006JF000664

Turcotte, D. L., & Schubert, G. (2014). *Geodynamics* (3rd ed.), Cambridge University Press.

Van der Veen, C. J. (1998). Fracture mechanics approach to penetration of bottom crevasses on glaciers. *Cold Regions Science and Technology*, *27*(3), 213–223. https://doi.org/10.1016/s0165-232x(98)00006-8
Watts, A. B. (2001). *Isostasy and flexure of the Lithosphere*. Cambridge University Press (ISBN: 0-521-622727).
Weertman, J. (1973). Can a water-filled crevasse reach the bottom surface of a glacier? In *Symposium on the Hydrology of Glaciers, Cambridge, 7–13, September 1969* (pp. 139–145). International Association of Hydrologic Sciences.
Weertman, J. (1980). Bottom crevasses. *Journal of Glaciology*, *25*. https://doi.org/10.3189/S0022143000010418